Journal of ELECTRONIC MATERIALS, Vol. 44, No. 6, 2015
DOI: 10.1007/s11664-015-3642-7

Evaluation of Electroplated Co-P Film as Diffusion Barrier Between In-48Sn Solder and SiC-Dispersed Bi_2Te_3 Thermoelectric Material

SIYANG LI,[1] DONGHUA YANG,[1] QING TAN,[1] and LIANGLIANG LI[1,2]

1.—State Key Laboratory of New Ceramics and Fine Processing, School of Materials Science and Engineering, Tsinghua University, Beijing 100084, People's Republic of China. 2.—e-mail: liliangliang@mail.tsinghua.edu.cn

The diffusion barrier property of Co-P film as a buffer layer between SiC-dispersed Bi_2Te_3 bulk material and In-48Sn solder was investigated. A Co-P film with thickness of ~6 μm was electroplated on SiC-dispersed Bi_2Te_3 substrate, joined with In-48Sn solder by a reflow process, and annealed at 100°C for up to 625 h. The formation and growth kinetics of intermetallic compounds (IMCs) at the interface between the In-48Sn and substrate were studied using transmission electron microscopy and scanning electron microscopy with energy-dispersive x-ray spectroscopy. The results showed that crystalline $Co(In,Sn)_3$ formed as an irregular layer adjacent to the solder side at the solder/Co-P interface due to diffusion of Co towards the solder, and a small amount of amorphous $Co_{45}P_{13}In_{12}Sn_{30}$ appeared at the Co-P side because of diffusion of In and Sn into Co-P. The growth of $Co(In,Sn)_3$ and $Co_{45}P_{13}In_{12}Sn_{30}$ during solid-state aging was slow, being controlled by interfacial reaction and diffusion, respectively. For comparison, In-48Sn/Bi_2Te_3-SiC joints were prepared and the IMCs in the joints analyzed. Without a diffusion barrier, In penetrated rapidly into the substrate, which led to the formation of amorphous In_xBi_y phase in crystalline In_4Te_3 matrix. These IMCs grew quickly with prolongation of the annealing time, and their growth was governed by volume diffusion of elements. The experimental data demonstrate that electroplated Co-P film is an effective diffusion barrier for use in Bi_2Te_3-based thermoelectric modules.

Key words: In-Sn, Co-P, diffusion barrier, thermoelectric device, Bi_2Te_3

INTRODUCTION

Recently, thermoelectric (TE) devices have received increasing attention because they can directly convert heat to electricity and vice versa.[1–8] Bi_2Te_3 has an excellent figure of merit of ~1.0 near room temperature, and thus Bi_2Te_3-based TE devices have been used in portable power generators, refrigerators, and infrared sensors.[9–11] The efficiency of TE devices not only depends on the intrinsic properties of the TE materials, but also relies on the connections between the electrodes and TE materials.[12–14] The requirements for such connections are low stress, low contact resistance, and slow interdiffusion.[15–18] Intermetallic compounds (IMCs) always form between electrodes and TE materials, playing an important role in the efficiency and reliability of TE devices; therefore, it is important to study the formation and growth of IMCs.[15,19,20]

A diffusion barrier is typically required between electrodes and TE materials to enhance joint reliability and device efficiency. Various diffusion barriers have been investigated, including nitrides, noble metal, Ta, Ni, Co, Cr, and Mo.[21–30] Ni-based barriers have been widely used in commercial devices, and they are reliable diffusion barriers with low contact resistance of 10^{-6} Ω cm^2,[16,17,31] but Ni itself can diffuse into Bi_2Te_3-based materials, which

(Received May 31, 2014; accepted January 12, 2015; published online January 30, 2015)

degrades the performance of TE devices.[25,32] Electroless multilayered Ni-P/Co-P has been reported to be an effective diffusion barrier between Sn and Te, as the Co-P layer can prevent diffusion of Ni, but the fabrication of the multilayered structure is complex.[33] A single electroplated Co-P layer has shown a superior diffusion barrier property in preventing diffusion of Sn, and electrolytic plating has many advantages over electroless plating, such as selected-area deposition, high deposition rate, and flexible microstructure tuning.[28,34–36]

Solders are widely used electrode materials. Various solders, such as Sn-Bi, Sn-Ag-Cu, Sn-Pb, etc., have been investigated to join TE materials.[18,25,32,37–39] Lead-free In-48Sn solder has the advantages of low melting temperature (118°C), high ductility, good fatigue properties, and good wettability on various substrates, making In-48Sn a possible candidate for use in near-room-temperature TE devices.[40] However, there is little study on the application of In-48Sn solder in TE devices.

The purpose of this work is to investigate the IMCs in In-48Sn/Bi_2Te_3 connections and the diffusion barrier property of electroplated Co-P film as a buffer layer between In-48Sn solder and Bi_2Te_3 bulk material. Using SiC-dispersed Bi_2Te_3 as substrate, we prepared In-48Sn/Bi_2Te_3-SiC and In-48Sn/Co-P/Bi_2Te_3-SiC joints and systematically studied the IMCs and interfacial reactions in these joints during solid-state aging. In addition, the growth kinetics of IMCs was analyzed and the coefficients of the IMC growth rate were calculated.

EXPERIMENTAL PROCEDURES

Bulk SiC-dispersed Bi_2Te_3 was used as substrate. Adoption of SiC is helpful for enhancement of the thermoelectric and mechanical properties of Bi_2Te_3.[11,41] Commercial high-purity powders of Bi (99.99%, 100 mesh), Te (99.99%, 100 mesh), and SiC (99%) with average size of 30 μm were used as raw materials. These powders with chemical composition of Bi_2Te_3 with 0.5 vol.% SiC were subjected to a mechanical alloying (MA) process at 450 rpm for 3 h in a purified argon atmosphere.[41] Subsequently, the MAed powders were sintered using spark plasma sintering technology at axial compressive stress of 50 MPa and sintering temperature of 420°C. The sintered specimens were cut into small pieces and used as substrates. The substrate surface was polished using sandpapers, etched in 50 vol.% HNO_3 solution for 10 s to remove inorganic impurities and surface oxide, and finally cleaned with deionized water.

Co-P film was electroplated on SiC-dispersed Bi_2Te_3 substrates in an ultrasonic bath at ultrasonic power of 40 W and 70 ± 2°C.[28,36] The deposition was carried out under a positive current density of ~100 mA cm^{-2} and a negative current density of ~10 mA cm^{-2}. The working times of the positive and negative currents were 100 ms and 10 ms, respectively. The concentrations of $CoCl_2 \cdot 6H_2O$, $CoCO_3$, H_3PO_4, and H_3PO_3 were 200 g/L, 3.1 g/L, 5.5 g/L, and 5.5 g/L, respectively. The thickness of the Co-P layer was 6.2 ± 0.5 μm with 10 min plating. In-48Sn solder foil (52 wt.% In and 48 wt.% Sn, Indalloy® no. 1E; Indium Corporation) was joined with Bi_2Te_3-SiC and Co-P/Bi_2Te_3-SiC substrates by a reflow process in a reflow oven (lead-free reflow oven T200N+; Beijing Torch Technology). The peak temperature was 166°C. TACFlux® 055 (Indium Corporation) was used as soldering flux. After reflow, the samples were embedded in epoxy and polished using sandpapers and 50-nm colloidal silica for cross-sectional analysis under SEM. Solid-state aging was performed in a convection oven at 100°C for 100 h, 225 h, 400 h, and 625 h in air.

Backscattered scanning electron microscopy (SEM, FEI Quanta 200 FEG) was applied to observe the interfacial IMCs in the samples. The IMC thickness was calculated by dividing the IMC area by the length of the SEM image. Images at multiple locations were used to improve the statistical accuracy and obtain the average thickness. The phase and composition of Co-P films and IMCs were determined by transmission electron microscopy (TEM, JEOL JEM-2100) and energy-dispersive x-ray spectroscopy (EDS). TEM specimens were cut at selected locations of SEM samples using the focused ion beam technique (FIB, TESCAN LYRA 3).

RESULTS AND DISCUSSION

In-48Sn/Bi_2Te_3-SiC Joints

Figure 1 presents cross-sectional SEM images at the interfaces of In-48Sn/Bi_2Te_3-SiC specimens annealed at 100°C for 0 h, 100 h, 225 h, 400 h, and 625 h. An IMC layer with average thickness of 5 μm was clearly observed at the interface after the reflow process (0 h). The thickness of the IMC layer rapidly increased with prolongation of the annealing time, reaching 11 μm on average after 625 h.

To study the composition of IMCs and diffusion, EDS elemental mapping analysis and line scanning were carried out. Figure 2a illustrates the morphology of IMCs at the interface of the In-48Sn/Bi_2Te_3-SiC joint annealed at 100°C for 625 h, and Fig. 2b shows the compositional profiles of In, Sn, Te, and Bi along the line perpendicular to the interface of the joint. It was found that indium penetrated rapidly into the substrate, whereas Sn diffused rarely. The EDS elemental mapping images in Fig. 2c and d show the distribution of In and Sn, respectively, confirming fast diffusion of In and rare diffusion of Sn.

To identify interfacial IMCs, TEM characterization was carried out. Figure 3a shows the microstructure of two kinds of IMC. One was In_xBi_y, and the other was In_4Te_3. The composition of In_xBi_y was obtained by

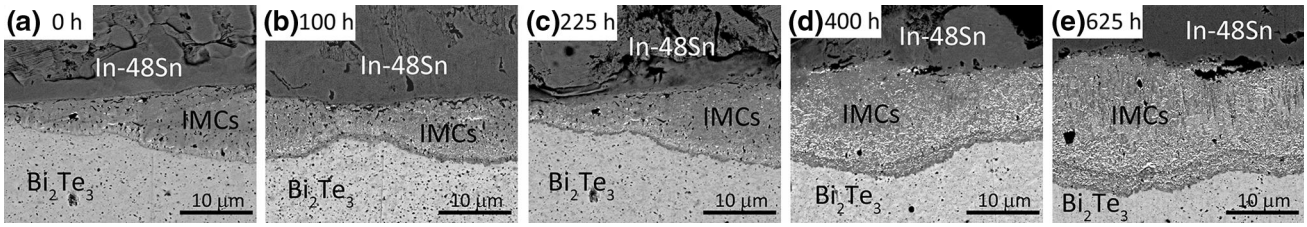

Fig. 1. Cross-sectional SEM images of In-48Sn/Bi_2Te_3-SiC joints annealed at 100°C for (a) 0 h, (b) 100 h, (c) 225 h, (d) 400 h, and (e) 625 h.

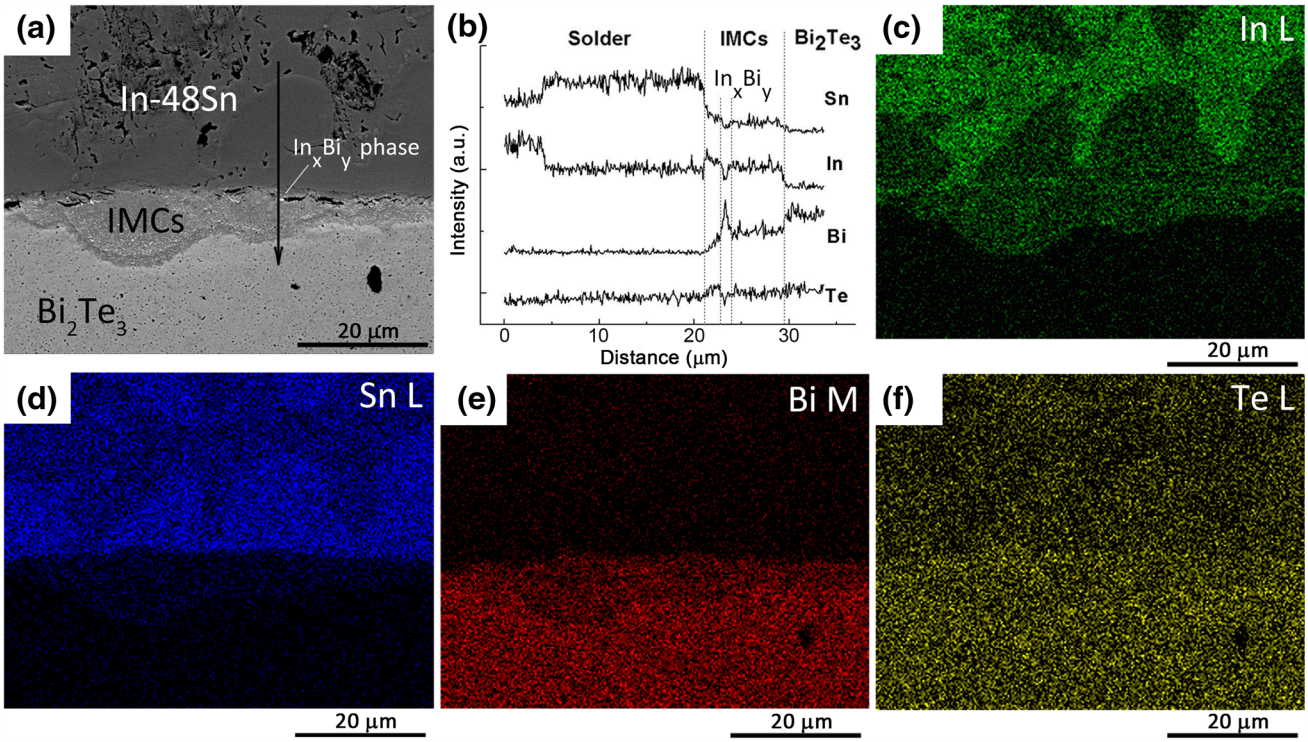

Fig. 2. Elemental mapping analysis of In-48Sn/Bi_2Te_3-SiC annealed at 100°C for 625 h: (a) morphology at the interfaces, (b) compositional profile, and elemental maps of (c) In, (d) Sn, (e) Bi, and (f) Te.

TEM-EDS. The value of x was in the range from 30 to 45, and y was in the range from 55 to 70. The selected-area electron diffraction (SAED) pattern of In_xBi_y in Fig. 3b clearly shows indistinct rings, indicating that this phase is amorphous. The SAED pattern in Fig. 3c shows that In_4Te_3 was crystalline. The indexing results for In_4Te_3 are labeled according to Joint Committee on Powder Diffraction Standards (JCPDS) file no. 83-0040. The SEM images in Fig. 4 show the distribution of In_xBi_y and In_4Te_3. In_xBi_y appears white in Fig. 4a and b, and it may gather to form a cluster or disperse in the matrix of In_4Te_3.

The growth of an IMC layer may be described by a power law:

$$\ln(x - x_0) = n \ln t + \ln k, \quad (1)$$

where x is the thickness of IMC, x_0 is the initial thickness before the aging process, k is the growth rate constant, t is the annealing time, and n is an exponent.[42] The thickness of the IMC layer as a function of annealing time is plotted in Fig. 5. n and k were calculated as 0.54 and 4.3×10^{-3} $\mu m\ s^{-1/2}$, respectively. Because the n value is very close to 0.5, the growth of the IMC layer was governed by volume diffusion.[42] The fast formation of IMCs caused by diffusion of In-48Sn may result in degradation of various properties and the reliability of joints between solder and substrate.[38,43,44] We will perform further investigation in future work, especially on the mechanical properties of the joints.

In-48Sn/Co-P/Bi_2Te_3-SiC Joints

We deposited a Co-P film with P content of 8.0 ± 1.1 at.% on Bi_2Te_3-SiC substrate. Figure 6a shows the interfacial morphology of the In-48Sn/

Co-P/Bi_2Te_3-SiC joint annealed at 100°C for 400 h. It is clear that diffusion of In-48Sn was blocked by the Co-P film. No obvious interdiffusion between Co-P and Bi_2Te_3 was observed under SEM. Figure 6b presents the compositional line profile according to the arrow in Fig. 6a. Elemental maps for Sn, In, Co, P, Bi, and Te are shown in Fig. 6c–h, respectively. The false appearance of Te at the solder side in Fig. 6h is due to interference from the Sn signal (L spectral line) in the EDS measurement. Two kinds of IMC were observed. One IMC with composition $Co_xIn_ySn_y$ formed and grew irregularly on the solder side at the interface due to diffusion of Co from the Co-P film to the solder. The value of x was in the range from 24 to 26, y in the range from 10 to 13, and z in the range from 59 to 64. The other IMC was adjacent to the Co-P film; its composition was $Co_{45}P_{13}In_{12}Sn_{30}$, being caused by diffusion of In and Sn into Co-P.

The TEM image in Fig. 7a shows the morphology at the interface between solder and Co-P. The SAED pattern of region A indicates $CoSn_3$-type crystalline IMC (JCPDS file no. 48-1813), as shown in Fig. 7b. Because some In atoms were dissolved into the $CoSn_3$ lattice, this IMC was identified as $Co(In,Sn)_3$, which was also consistent with the compositional analysis by SEM-EDS. The SAED pattern of region B in Fig. 7c, which corresponds to $Co_{45}P_{13}In_{12}Sn_{30}$ IMC, shows indistinct rings that are characteristic of amorphous structure. Figure 7d shows a high-resolution TEM image of local region D. Lattice fringes can be observed for $Co(In,Sn)_3$ but not for $Co_{45}P_{13}In_{12}Sn_{30}$, confirming that $Co(In,Sn)_3$ is crystalline and $Co_{45}P_{13}In_{12}Sn_{30}$ is amorphous. In addition, the indexing results in

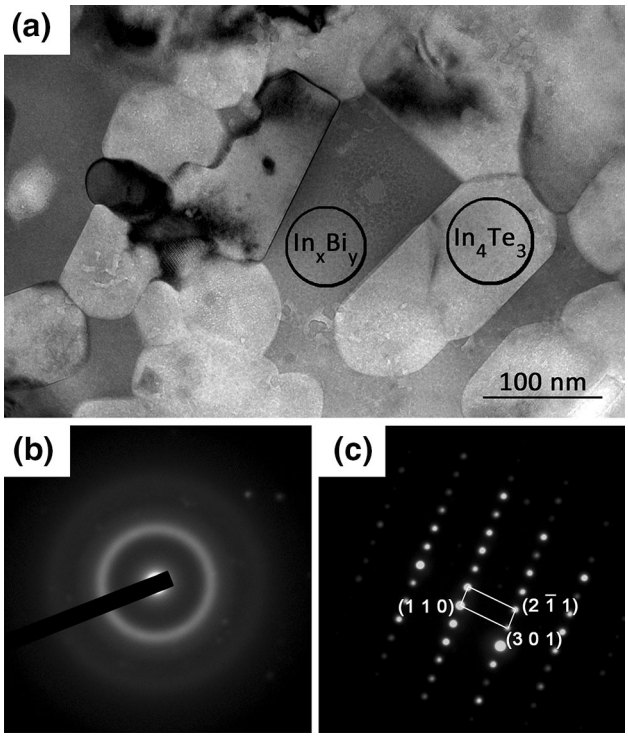

Fig. 3. TEM analysis of In_xBi_y and In_4Te_3 IMCs: (a) microstructure, and SAED patterns of (b) In_xBi_y and (c) In_4Te_3.

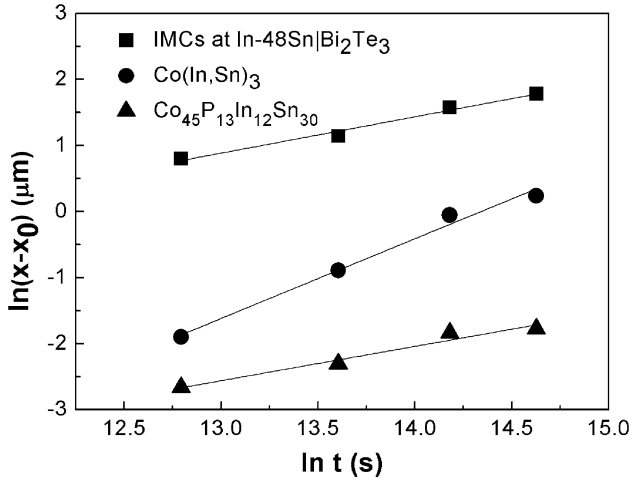

Fig. 5. Plots of growth of IMCs in In-48Sn/Bi_2Te_3-SiC and In-48Sn/Co-P/Bi_2Te_3-SiC joints.

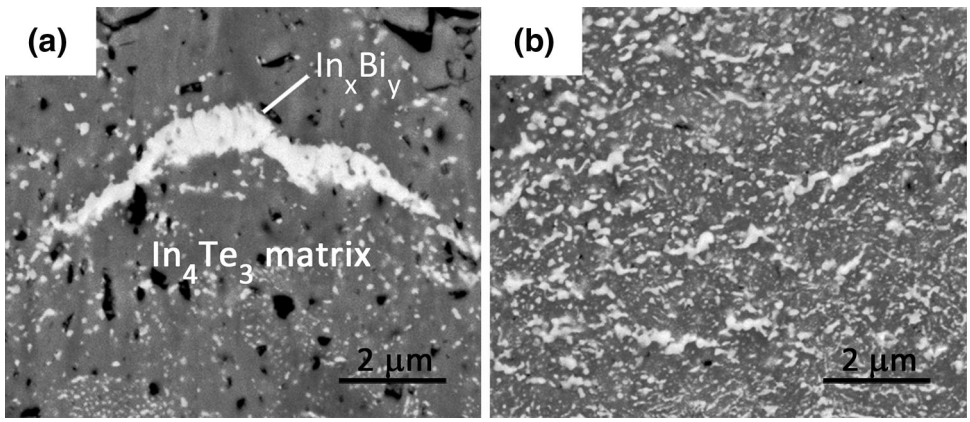

Fig. 4. (a) Gathered In_xBi_y phase, and (b) dispersed In_xBi_y phase in In_4Te_3 matrix.

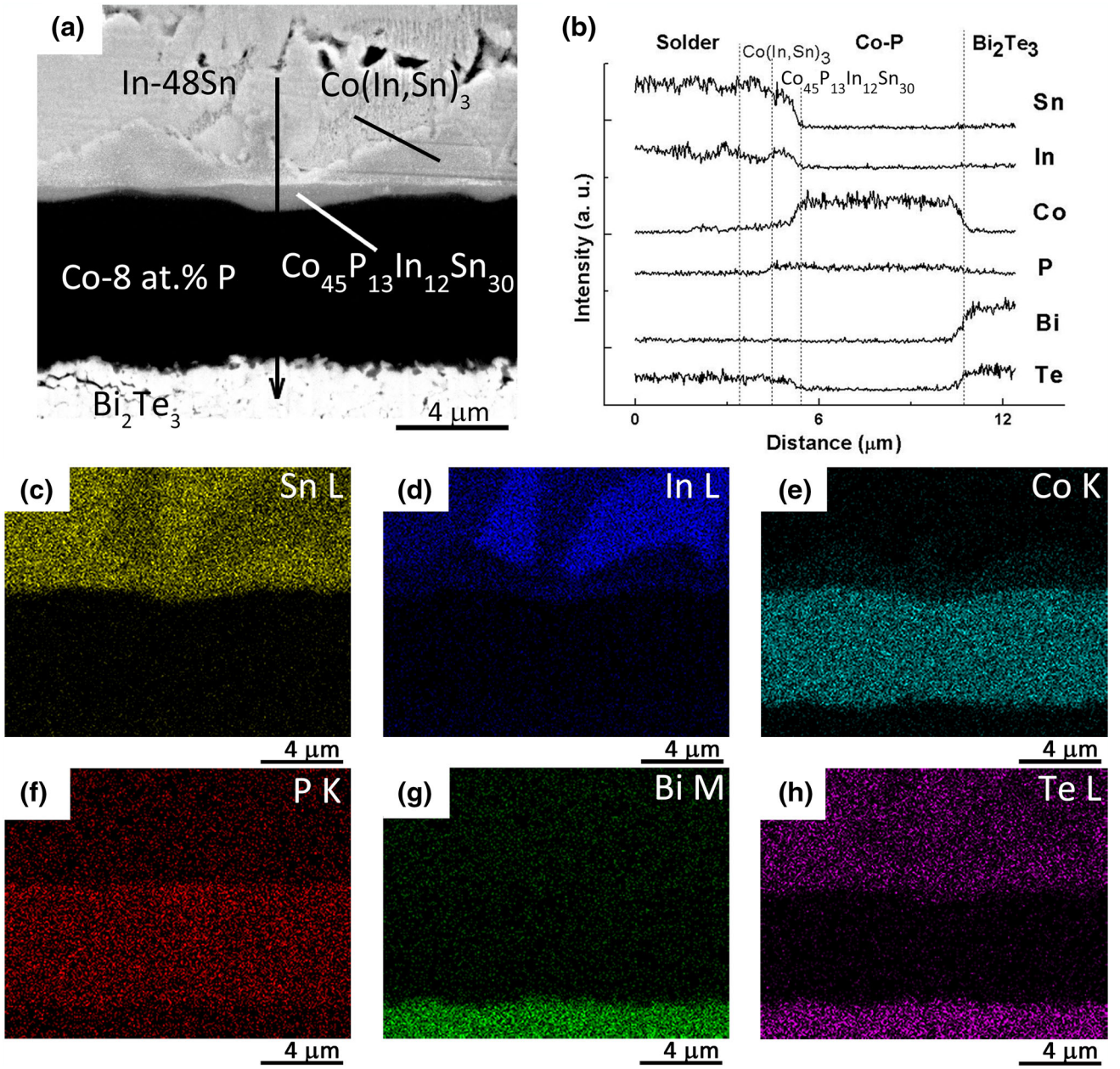

Fig. 6. Elemental mapping analysis of In-48Sn/Co-P/Bi_2Te_3-SiC annealed at 100°C for 400 h: (a) morphology at the interfaces, (b) compositional profile, and elemental maps of (c) Sn, (d) In, (e) Co, (f) P, (g) Bi, and (h) Te.

Fig. 7e show that the Co-P film (region C) has hexagonal close-packed (hcp) Co-type crystal structure (JCPDS file no. 05-0727).

Figure 8 shows the evolution of the interfacial IMCs between In-48Sn solder and Co-P film annealed at 100°C from 0 h to 625 h. Both $Co(In,Sn)_3$ and $Co_{45}P_{13}In_{12}Sn_{30}$ IMCs grew nonuniformly at the interface. The thicknesses of both IMCs increased with prolongation of the aging time. The average thicknesses of $Co(In,Sn)_3$ and $Co_{45}P_{13}In_{12}Sn_{30}$ obtained from multiple locations are plotted as a function of annealing time in Fig. 5. The n value for $Co(In,Sn)_3$ were calculated to be 1.21 and 6×10^{-7} $\mu m\ s^{-1}$ according to Eq. 1, respectively. Because the n value for $Co(In,Sn)_3$ is close to 1.0, the growth of $Co(In,Sn)_3$ was governed by interfacial reaction. In contrast, the n and k values for $Co_{45}P_{13}In_{12}Sn_{30}$ were calculated to be 0.52 and 1×10^{-4} $\mu m\ s^{-1/2}$. $Co_{45}P_{13}In_{12}Sn_{30}$ has an n value close to 0.5, meaning that its growth was controlled by volume diffusion at the interface.[42] After 625 h, the thicknesses of $Co(In,Sn)_3$ and $Co_{45}P_{13}In_{12}Sn_{30}$ IMCs were 1.89 μm and 0.26 μm, respectively. The growth of these two IMCs was much slower than that of the IMCs formed in In-48Sn/Bi_2Te_3-SiC joints. Therefore, Co-P is a very effective diffusion barrier for both In and Sn.

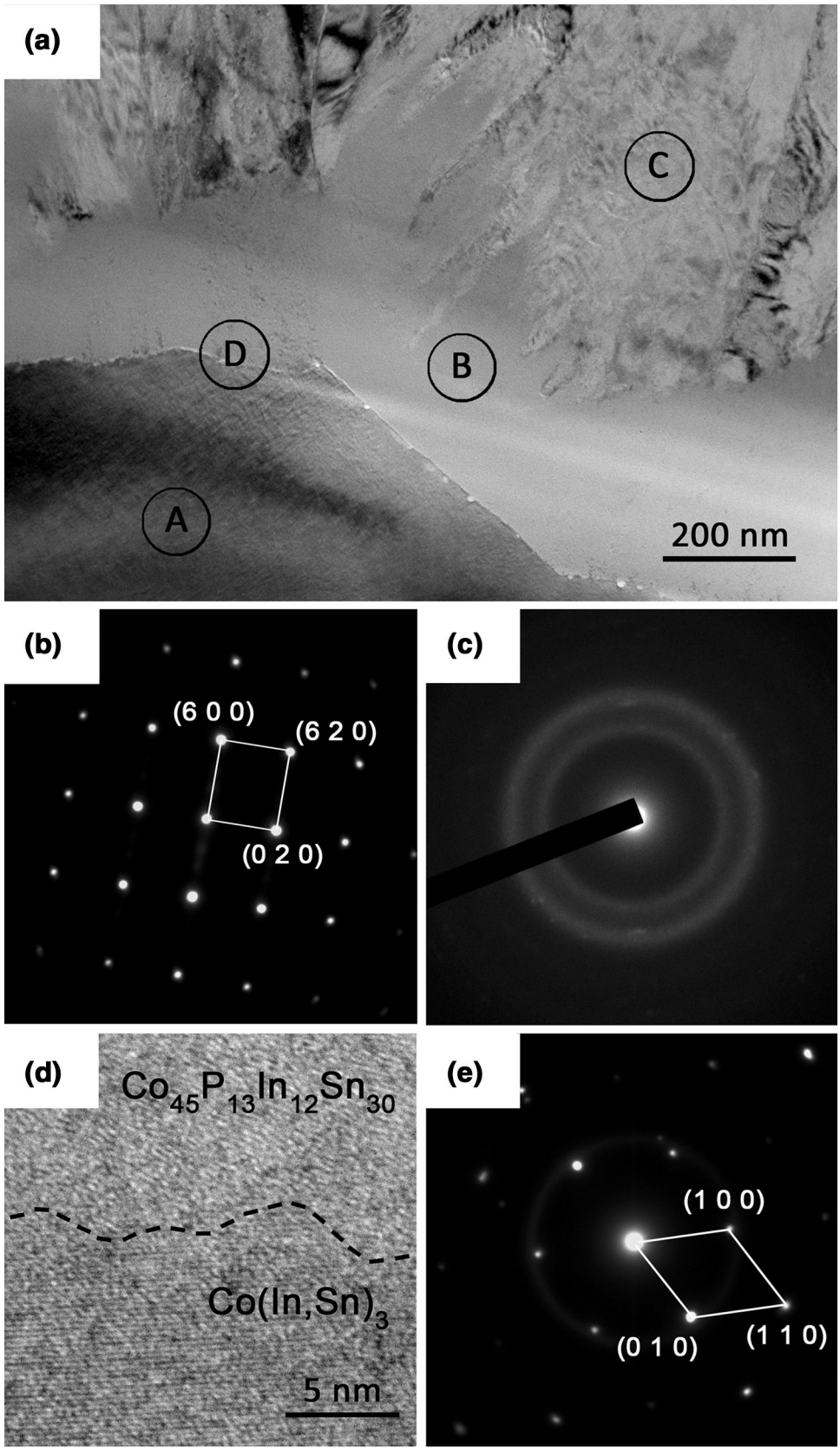

Fig. 7. TEM analysis of IMCs at the interface between solder and Co-P: (a) interfacial morphology, (b) SAED pattern of $Co(In,Sn)_3$ in region A, (c) SAED pattern of $Co_{45}P_{13}In_{12}Sn_{30}$ in region B, (d) high-resolution TEM image at the interface between amorphous $Co_{45}P_{13}In_{12}Sn_{30}$ and crystalline $Co(In,Sn)_3$ in region D, and (e) SAED pattern of Co-P in region C.

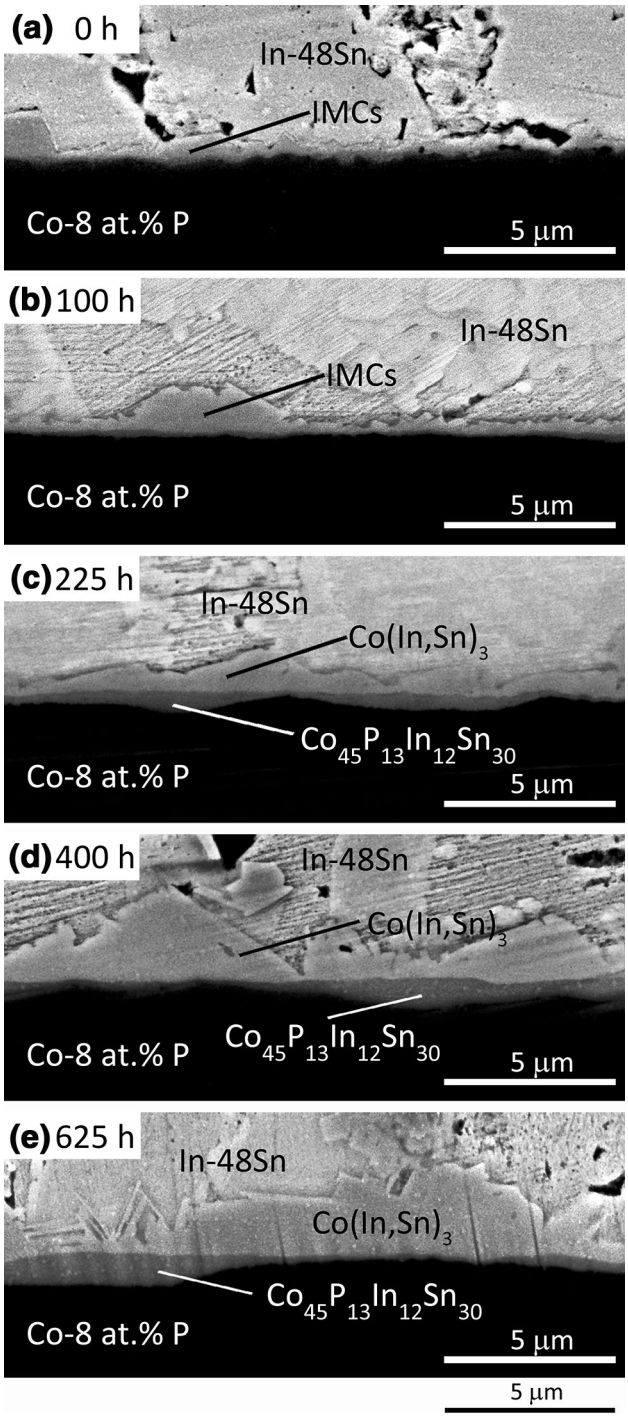

Fig. 8. Cross-sectional SEM images at In-48Sn/Co-P interfaces annealed at 100°C for (a) 0 h, (b) 100 h, (c) 225 h, (d) 400 h, and (e) 625 h.

CONCLUSIONS

We studied the interfacial reaction of In-48Sn solder with SiC-dispersed Bi_2Te_3 and evaluated electroplated Co-P film as a diffusion barrier for In-48Sn. Without a diffusion barrier, In diffused rapidly into the substrate, leading to the formation of amorphous In_xBi_y and crystalline In_4Te_3 phases. These IMCs grew quickly and reached 11 μm on average after an annealing process at 100°C for 625 h. In contrast, a Co-P film with thickness of 6 μm effectively bonded solder with substrate and blocked diffusion of In and Sn. The thicknesses of crystalline $Co(In,Sn)_3$ and amorphous $Co_{45}P_{13}In_{12}Sn_{30}$ IMCs that formed between the solder and Co-P film increased to 1.89 μm and 0.26 μm after 625 h annealing, respectively. The experimental data demonstrate that Co-P is an effective diffusion barrier for use with In-48Sn solder in Bi_2Te_3-based TE devices.

ACKNOWLEDGEMENTS

This work was supported by the National Basic Research Program of China (Grant No. 2013CB632504) and the National Natural Science Foundation of China (Grant No. 51102149). We thank Prof. Jing-Feng Li for help with synthesis of SiC-dispersed Bi_2Te_3 material.

REFERENCES

1. M. Mizoshiri, M. Mikami, K. Ozaki, and K. Kobayashi, *J. Electron. Mater.* 41, 1713 (2012).
2. B. Poudel, Q. Hao, Y. Ma, Y.C. Lan, A. Minnich, B. Yu, X. Yan, D.Z. Wang, A. Muto, D. Vashaee, X.Y. Chen, J.M. Liu, M.S. Dresselhaus, G. Chen, and Z. Ren, *Science* 320, 634 (2008).
3. G.J. Snyder, J.R. Lim, C.K. Huang, and J.P. Fleurial, *Nat. Mater.* 2, 528 (2003).
4. L.M. Goncalves, C. Couto, P. Alpuim, and J.H. Correia, *J. Micromech. Microeng.* 18, 064008 (2008).
5. I. Chowdhury, R. Prasher, K. Lofgreen, G. Chrysler, S. Narasimhan, R. Mahajan, D. Koester, R. Alley, and R. Venkatasubramanian, *Nat. Nanotech.* 4, 235 (2008).
6. D. Xu, B. Xiong, and Y. Wang, *Smart Mater. Struct.* 20, 015013 (2011).
7. Y. Zhou, L.L. Li, Q. Tan, and J.F. Li, *J. Alloys Compd.* 590, 362 (2014).
8. D. Li, L. Li, D.W. Liu, and J.F. Li, *Phys. Status Solidi RRL* 6, 268 (2012).
9. Z. Wang, V. Leonov, P. Fiorini, and C. Van Hoof, *Sens. Actuators A* 156, 95 (2009).
10. R. Funahashi, M. Mikami, T. Mihara, S. Urata, and N. Ando, *J. Appl. Phys.* 99, 066117 (2006).
11. D.W. Liu, J.F. Li, C. Chen, B.P. Zhang, and L.L. Li, *J. Micromech. Microeng.* 20, 125031 (2010).
12. L.W. Da Silva and M. Kaviany, *Int. J. Heat Mass. Transf.* 47, 2417 (2004).
13. G. Min and D.M. Rowe, *Energy Convers. Manag.* 41, 163 (2000).
14. A.M. Pettes, R. Melamud, S. Higuchi, and K.E. Goodson, *Proceedings of the 26th International Conference on Thermoelectrics*, Jeju Island, South Korea (2007), p. 283.
15. M.T. Barako, W. Park, A.M. Marconnet, M. Asheghi, and K.E. Goodson, *J. Electron. Mater.* 42, 372 (2013).
16. R.P. Gupta, K. Xiong, J.B. White, K. Cho, H.N. Alshareef, and B.E. Gnade, *J. Electrochem. Soc.* 157, H666 (2010).
17. K. Xiong, W. Wang, H.N. Alshareef, R.P. Gupta, J.B. White, B.E. Gnade, and K. Cho, *J. Phys. D Appl. Phys.* 43, 115303 (2010).
18. C.L. Yang, H.J. Lai, J.D. Hwang, and T.H. Chuang, *J. Electron. Mater.* 42, 359 (2013).
19. W.P. Lin, D.E. Wesolowski, and C.C. Lee, *J. Mater. Sci.: Mater. Electron.* 22, 1313 (2011).
20. R.P. Gupta, O.D. Iyore, K. Xiong, J.B. White, K. Cho, H.N. Alshareef, and B.E. Gnade, *Electrochem. Solid-State Lett.* 12, H395 (2009).

21. T. Kacsich, E. Kolawa, J.P. Fleurial, T. Caillat, and M.A. Nicolet, *J. Phys. D Appl. Phys.* 31, 2406 (1998).
22. N.H. Bae, S. Han, K.E. Lee, B. Kim, and S.T. Kim, *Curr. Appl. Phys.* 11, S40 (2011).
23. O.D. Iyore, T.H. Lee, R.P. Gupta, J.B. White, H.N. Alshareef, M.J. Kim, and B.E. Gnade, *Surf. Interface Anal.* 41, 440 (2009).
24. R. Zybała, K.T. Wojciechowski, M. Schmidt, and R. Mania, *Materiały Ceramiczne/Ceram. Mater.* 62, 481 (2010).
25. T.Y. Lin, C.N. Liao, and A.T. Wu, *J. Electron. Mater.* 41, 153 (2012).
26. H.H. Hsu, C.H. Cheng, Y.L. Lin, S.H. Chiou, C.H. Huang, and C.P. Cheng, *Appl. Phys. Lett.* 103, 053902 (2013).
27. S.P. Feng, Y.H. Chang, J. Yang, B. Poudel, B. Yu, Z. Ren, and G. Chen, *Phys. Chem. Chem. Phys.* 15, 6757 (2013).
28. N.D. Lu, D.H. Yang, and L.L. Li, *Acta Mater.* 61, 4581 (2013).
29. H. Ono, T. Nakano, and T. Ohta, *Appl. Phys. Lett.* 64, 1511 (1994).
30. T.N. Arunagiri, Y. Zhang, O. Chyan, M. EI-Bouanani, M.J. Kim, K.H. Chen, C.T. Wu, and L.C. Chen, *Appl. Phys. Lett.* 86, 083104 (2005).
31. D.M. Rowe, *CRC Handbook of Thermoelectrics* (Boca Raton: CRC Press, 1995).
32. Y.C. Lan, D.Z. Wang, G. Chen, and Z.F. Ren, *Appl. Phys. Lett.* 92, 101910 (2008).
33. C.Y. Ko and A.T. Wu, *J. Electron. Mater.* 41, 3320 (2012).
34. Y.C. Lin and J.G. Duh, *J. Alloys Compd.* 439, 74 (2006).
35. N. Lu, Y. Li, J. Cai, and L. Li, *IEEE Trans. Magn.* 47, 3799 (2011).
36. N. Lu, J. Cai, and L. Li, *Surf. Coat. Technol.* 206, 4822 (2012).
37. L. Shen, F. Guo, N. Zheng, and R. Zhao, *Proceedings of 13th International Conference on Electronic Packaging Technology and High Density Packaging*, Guilin, China (2012), p. 1578.
38. C.N. Liao, C.H. Lee, and W.J. Chen, *Electrochem. Solid-State Lett.* 10, 23 (2007).
39. W.P. Lin and C.C. Lee, *IEEE Trans. Compon. Packag. Manuf. Technol.* 1, 1311 (2011).
40. S.W. Chen, C.H. Wang, S.K. Lin, and C.N. Chiu, *J. Mater. Sci.: Mater. Electron.* 18, 19 (2007).
41. L.D. Zhao, B.P. Zhang, J.F. Li, M. Zhou, W.S. Liu, and J. Liu, *J. Alloys Compd.* 455, 259 (2008).
42. H. Schmalzried, *Chemical Kinetics of Solids*, VCH (2008).
43. J. Koo and S. Jung, *J. Electron. Mater.* 34, 1565 (2005).
44. J. Koo and S. Jung, *Mater. Sci. Eng. A* 397, 145 (2005).